Long noncoding RNA NEAT1 regulates glioma cells proliferation and apoptosis by competitively binding with miR-324-5p and upregulating KCTD20 expression

Jiale Zhang
Fourth Military Medical University
Yangyang Li
Jiangsu Province Hospital and Nanjing Medical University First Affiliated Hospital
Yuqi Liu
Fourth Military Medical University
Guangzhi Xu
Fourth Military Medical University
Yue Hei
Fourth Military Medical University
Xiaoming Lu (luxm923@126.com)
Jiangsu Province Hospital and Nanjing Medical University First Affiliated Hospital
Liu Weiping (neurosurgeonliu@163.com)
Fourth Military Medical University https://orcid.org/0000-0002-8118-300X

Primary research

Keywords: Glioma, NEAT1, proliferation, apoptosis, miR-324-5p, KCTD20

Posted Date: May 18th, 2020

DOI: https://doi.org/10.21203/rs.3.rs-28541/v1

Abstract

Background

Recent studies have pointed out that long non-coding RNAs (lncRNAs) play a key role in tumorigenesis, including glioma. Nuclear paraspeckle assembly transcript 1 (NEAT1), a lncRNA, has been reported to be participated in the development and progression of many types of tumors and promotes cancer cell proliferation, migration, invasion, and drug resistance. The exact role and regulatory mechanism of NEAT1 in gliomas still need to be further explored.

Methods

NEAT1 expression was detected in paired glioma tissues and adjacent normal tissues, as well as in glioma cell lines by quantitative real-time PCR (qRT-PCR). Cell viability and apoptosis were measured using flow cytometry, colony formation assays and TdT-mediated dUTP nick-end labeling (TUNEL) assay. The mechanism of competing endogenous RNA (ceRNA) between NEAT1 and miR-324-5p was determined using bioinformatics analysis, RIP and luciferase reporter assay.

Results

Here we demonstrated that lncRNA NEAT1 was upregulated and significantly associated with poor prognosis in glioma tissues. Through gain- and loss-of NEAT1 expression, we found that knockdown of NEAT1 inhibited the abilities of cell proliferation and induced G0/G1 arrest and apoptosis in vitro, suppressed tumorigenesis in vivo via sponging miR-324-5p and then upregulated KCTD20 expression. In addition, NEAT1 reversed the effects of miR-324-5p on the proliferation and apoptosis of glioma cells, and involved the inhibition of potassium channel tetramerization protein domain containing 20 (KCTD20) expression.

Conclusion

Collectively, our findings demonstrate that NEAT1 epigenetically up-regulates KCTD20 expression through competitively binding miR-324-5p, and also provides a potential therapeutic target for human glioma.

Background

Glioma, the most prevalent and aggressive tumor in the central nervous system, is accounting for 70% of highly malignant primary brain tumors(1). Despite the constantly improving multiple diagnosis and treatment strategies in past decades including surgical resection followed by radiotherapy and systemic Temozolomide (TMZ) chemotherapy(2), the prognosis for patients with glioma remains dismal, and the overall survival is only 12–14 months after diagnosis (3, 4). In order to treat malignant gliomas more

efficiently, approaches have been performed to find molecular targets related with glioma cell growth, apoptosis, differentiation, invasion, and migration. However, developing effective targeted therapies to improve the cure rate for this complex disease remains a challenge. Therefore, it is urgent need to unveil the underlying mechanisms of gliomas, especially focusing on tumorigenesis and in order to develop more effective treatment strategies.

Long noncoding RNAs (lncRNAs), a subgroup of noncdoing RNAs, defined as ncRNAs with transcripts longer than 200 nucleotides and with little protein-coding potential(5, 6). The underlying regulatory mechanisms of lncRNAs function in cancer are very complex and not fully understood. Many studies have shown that lncRNA exerts a crucial role in role in the development process, genomic imprinting, cellular homeostasis, and pluripotency of embryonic stem cells(7–9). Generally, the abnormally expressed lncRNAs participate in many biological mechanisms at the epigenetic, transcriptional, and posttranscriptional levels(10–12), such as cell proliferation, metabolism, apoptosis, migration and differentiation(13–15). Recently, a new regulatory mechanism indicates that the potential effect of lncRNAs is to inhibit the expression and biological functions of miRNAs(microRNA) as competing endogenous RNAs (ceRNA)(16, 17). Emerging evidence has confirmed that ceRNA is a very important pathway in regulation of cancer progress, also known as sponge, which associate with miRNAs and regulates the miRNA downstream target genes. For instance, MT1JP regulated gastric cancer by functioning as competing endogenous RNA to regulate miR-92a-3p/FBXW7 expression(18). lncRNA TUSC8 served as a ceRNA of MYLIP through competitively binding with miR-190b-5p and inhibited breast cancer metastasis(19). Hence, there is no doubt that lncRNAs are the core factors in tumorigenesis and development, but the overall pathophysiological mechanism of lncRNAs in glioma remains to be determined.

The nuclear-enriched abundant transcript 1 (NEAT1), located on chromosome 11, has been reported to be a transcriptional regulator for numerous genes(20). Previous studies suggest that abnormal expression of NEAT1 promotes tumorigenesis in a variety of human cancers(21, 22). Furthermore, the lncRNA NEAT1 is involved in many tumors by acting as an endogenous competing RNA (ceRNA) for many tumor suppressor miRNAs(23). In non-small cell lung cancer, NEAT1 can promote the progression of NSCLC under hypoxic condition and regulate the Wnt/β-Catenin signaling pathway(24). Moreover, the overexpression of NEAT1 in pancreatic cancer was shown to facilitates cancer progression by negative modulation of miR-506-3p(25). Although there have been some articles on the regulation of NEAT1 in gliomas, few investigations involve intracranial tumor formation experiment. Therefore, we added the orthotopic xenograft studies experiment to this study, and selected NEAT1 to further study its regulation mode of proliferation and apoptosis in glioma.

In the current study, we determined that NEAT1 was upregulated in glioma tissues and cell lines and is closely correlated with the glioma progression and poor overall survival. Further mechanistic investigation has revealed that NEAT1 may function as ceRNA to compete with miR-324-5p via directly binding to KCTD20, which improved the expression levels of KCTD20. The inhibition of NEAT1 and KCTD20 significantly inhibited the proliferation of glioma cells, which was consistent with the results of

miR-324-5p overexpression. Our present work provides a novel understanding of the function of NEAT1/miR-324-5p/KCTD20 in the diagnosis and treatment of glioma patients.

Methods

Human Tissue Samples

All of the 43 paired human glioma tissues as well as the paired adjacent noncancerous tissues were obtained from patients who underwent surgical resection at from the Department of Neurosurgery, Jiangsu Province Hospital, the First Affiliated Hospital of Nanjing Medical University. Histologic grade was staged was classified by pathologists using WHO criteria. No surgical patients had received pre-operative radiotherapy or chemotherapy. All tissue samples were collected during surgery, frozen immediately in liquid nitrogen, and stored for total RNA or protein extraction. The clinical-pathological characteristics of the patients was summarized in Table 1. This study was approved by the Institutional Review Board and the ethics committee of Nanjing Medical University and Fourth Military Medical University, and informed consent was obtained from all patients.

Cell culture

Six human GBM cell lines U87, LN229, H4, U251, U118 and A172 and human embryonic kidney (HEK) 293T cells were obtained from Cell Bank of the Chinese Academy of Sciences (Shanghai, China). And all cells were sustained in Dulbecco's modified Eagle's medium (DMEM) supplemented with 10% fetal bovine serum (FBS), 100 U of penicillin/mL and 100 ng of streptomycin/mL at humidified air at 37℃ with 5% CO_2. NHA cells were purchased from Lonza (Walkersville, MD) and cultured in the provided astrocyte growth media supplemented with rhEGF, insulin, ascorbic acid, GA-1000, L-glutamine and, 5% FBS.

Total RNA extraction and quantitative RT-PCR assays

Total RNA was extracted from glioma tissues or cultured cell lines using TRIzol reagent (Invitrogen) according to the manufacturer's protocol. The quantitative real-time polymerase chain reaction (qRT-PCR) was performed using an Applied Biosystems 7900 Sequence Detection system. First-strand cDNA was synthesized using the Primerscript RT Master Mix (TaKaRa). The gene-specific primers used in qRT-PCR experiments were as follows: NEAT1: 5'-TGGCTAGCTCAGGGCTTCAG-3 and 5'-TCTCCTTGCCAAGCTTCCTTC-3'; miR-324-5p: 5'-CGCGGATCCGGGTGGATGTAAGGGATGAG-3' and 5'-CCGGAATTCTTGGGCTGATCCAGGAGAAG-3'; KCTD20: 5'-CGGGATCCATGAATGTTCACCGTGGCAG-3' and 5'-CGAATTCCTAATCC TGAAAGTCGTTAGAAGC-3'; GAPDH: 5'-GACTCATGA CCACAGTCCATGC-3' and 5'-AGAGGCAGGGATGATGTTCTG-3'. All the primers used for miRNA reverse transcription and qRT-PCR were purchased from RiboBio (Guangzhou, China). The relative expression levels of NEAT1 and KCTD20 were normalized to GAPDH, while U6 was used as an internal control for miRNA. The expression levels of NEAT1, miR-324-5p and KCTD20 were calculated by 2-ΔΔCt analysis.

Cell transfection

The NEAT1 (siNEAT1) and KCTD20 (siKCTD20), pcDNA3.1 plasmids, pcDNA-NEAT1 and empty vector, and the expression of miR-324-5p was achieved by transfection of miR-324-5p mimics or miR-324-5p inhibitor were synthesized by Genechem (Shanghai, China). For stable transfection, the lentivirus carrying short hairpin RNA designed against NEAT1 (shNEAT1), shKCTD20 and its negative control was packaged in GBM cells using the lentiviral packaging kit (Genechem Shanghai, China). All the plasmids were transfected into cells grown in DMEM culture media using Lipofectamine 3000 Transfection Reagent (Invitrogen, Carlsbad, CA) according to the manufacturer's instructions.

Cell proliferation assay

At 48 hours after transfection, cells were seeded at 2000 per well in 96-well plates and cultured. Firstly, cell proliferation rate was detected at the indicated time points (24, 48, 72 and 96h) using a Cell Counting Kit-8 (CCK8) assay (Dojindo, Japan) following the manufacturer's instructions. After a 1 h incubation with CCK-8 at 37 °C, absorbance (OD value) at a wave length of 450 nm was detected and used for calculating cell viability.

The colony formation assay was performed following the method described in our earlier study(26). Briefly, cells were harvested 24h after transfection and then seeded onto 6-well plate (200 cells/well). After cultured for approximately 2 weeks until colony formation was observed, visible colonies were fixed with 100% methanol and stained with 0.1% crystal violet for 15 minutes. Colony-forming efficiency was calculated as the number of colonies/plated cells ×100%.

For the 5-ethynyl-2-deoxyuridine (EdU) proliferation assay, the Cell-Light EdU labeling detection kit was purchased from Life Technologies (MA, USA), in accordance with the manufacturer's protocol. U251 and LN229 cells were transfected with plasmid DNA or siRNA for 48 hours. were incubated with 10 μM EdU for 24 h, fixed, permeabilized, and stained with both the Alexa-Fluor 594 reaction cocktail for the EdU, and DAPI was used to label cell nuclei. The EdU-positive cells were visualized using a fluorescence microscope.

TUNEL assay

The transfected GBM cell lines were fixed in 4% paraformaldehyde for 15 minutes and stained with In Situ Cell Death Detection Kit, POD (Roche, Switzerland) according to the manufacturer's instructions. Firstly, cells were incubated in terminal dexynucleotidyl transferase (TdT) reaction cocktail for 45 minutes at 37°C, then treated with Click-iT reaction cocktail. The nucleus was stained with hematoxylin or methyl green. Finally, the percentage of TUNEL-positive cells were observed with Nikon ECLIPSE E800 fluorescence microscope.

Flow cytometric analysis

Cell cycle analysis was performed as described previously(27). For cell cycle assays, U251 and LN229 cells that were transfected with indicated lentivirus and/or plasmids for 48 hours, and then collected by centrifugation for five minutes at 2000 r/minute. Next, cells were washed twice with PBS and fixed with

75% ice-cold ethanol for 24h. The collected cells were re-suspended in PBS containing 25 mg/ mL propidium iodide, 0.1% Triton, and 10 mg/mL RNase (Multi Sciences, Hangzhou, China) and incubated for 30 minutes in the dark before being analyzed by a flow cytometry.

The apoptotic cells were stained with Annexin V-FITC/ Propidium iodide (PI) and assessed by fluorescence activated cell sorting (FACS). Cells were divided into dead cells(B1), late apoptotic cells(B2), cells viable cells(B3), and early apoptotic(B4) according to different periods. In each experiment, the total percentage of early and late apoptotic cells was compared to controls.

Orthotopic xenograft studies

Male immunodeficient nude mice (6-weeks-old) were purchased from Shanghai Experimental Animal Centre of the Chinese Academy of Sciences. To examine tumor growth in the orthotopic xenograft model, U251 cells (2.5×10^5) were stably transfected with shNEAT1 or shKCTD20 and the corresponding negative control were injected intracranially into the striatum of NOD/SCID mice by a stereotactic device (coordinates: 2 mm anterior, 2 mm lateral, 3 mm depth from the dura). Bioluminescence imaging (IVIS Spectrum, PerkinElmer, USA) was used to confirm tumor formation and to measure tumor growth weekly. All animal experimental procedures were approved by the Fourth Military Medical University (Xi'an, China) Institutional Committee for Animal Research and were in accordance with the Animal Management Rule of the Chinese Ministry of Health (document 55, 2001).

Western blotting assay and antibodies

Western blot analysis was done as described previously(28). Briefly, cells in culture were lysed using the RIPA buffer (KenGEN, China). Next, total protein extraction was evaluated by BCA Protein Assay Kit (Pierce, Thermo Fisher Scientific). Equal amounts of the protein extracts were loaded, subjected to 10% SDS-PAGE, transferred onto PVDF membrane (Millipore, Billerica, MA, USA) for western blotting analysis. After blocking membranes with 5% non-fat for 2h, they were probed by antibodies against CDK4 (Abcam), Cyclin D1 (Abcam), Bcl-2 (Abcam), Bax(Abcam), KCTD20 (Abcam), and GAPDH (Santa Cruz) at 4 °C overnight. They were then incubated with corresponding secondary antibodies, and processed using enhanced chemiluminescence reagents. An enhanced chemiluminescence (ECL) detection system (Thermo Scientific, USA) was applied to visualize the protein. GAPDH was used as an internal control.

Fluorescence in situ hybridization (FISH) and immunohistochemistry (IHC) analysis

The lncRNA NEAT1 expression level in glioma tissues and normal samples was examined by fluorescence in situ hybridization (FISH). Probes against lncRNA NEAT1 were synthesized by GoodBio (Wuhan, China). FISH was performed according to the BioSense manufacturer's protocol. Frozen human samples were fixed with 4% paraformaldehyde for 30 minutes and then washed 3 times with PBS. Treated sections were digested with Proteinase K for 3 minutes at 37 °C and then sequentially dehydrated for 5 min in 70, 85, and 100% ethanol. Next, probes were denatured at 78 °C for 5 minutes and then hybridized with sections overnight in a humidification chamber at 42 °C. Tissue sections were washed

with preheated 2 × sodium citrate (SSC), 1 × SSC, and 0.5 × SSC in sequence at 37 ° C for 10 minutes. Then sections washed 3 times with PBS and stained with 4',6-diamidino-2-phe-nylindole (Sigma) for 15 minutes. They were then examined with a Zeiss LSM 700 confocal microscope (Oberkochen, Germany). lHC was performed on mice xenogeneic tumor tissue and human tissue as described previously(29).

RNA immunoprecipitation

RIP (RNA immunoprecipitation) assay was performed with the Magna RIP RNA-Binding Protein lmmunoprecipitation Kit (Millipore, Billerica, MA, USA) following the manufacturer's protocol. Briefly, U251 and LN229 cells lysates were prepared and incubated with RIP buffer containing magnetic beads conjugated with human anti-Argonaute2 (anti-Ago2) antibody, while normal mouse lgG functioned as a negative control. lmmuno-precipitated RNA was tested by qRT-PCR analysis to verify the presence of NEAT1 and miR-324-5p expressions detection.

Luciferase reporter assay

The complementary DNA fragment containing the wild type (WT) or mutant (MUT) sequences of NEAT1 or KCTD20 were subcloned downstream of the luciferase gene within the pGL3 vectors. Briefly, cells were seeded in a 24-well plate and co-transfected with either empty vector or miR-125a, miR-324-5p, miR-495-3p and miR-504, firefly luciferase reporter comprising wild-type or mutant NEAT1 and 3'UTR of KCTD20 fragment using Lipofectamine 2000 (lnvitrogen) according to the protocol. At 48 h after transfection, the relative luciferase activities were measured using a dual luciferase assay kit (Promega, Madison, WI, USA). The relative luciferase activity was normalized against to the Renilla luciferase activity. All experiments were performed in triplicate.

Bioinformatic analyses

The database of glioma bioinformatics analysis among The Cancer Genome Atlas (TCGA)(Data Portal http://cancergenome. nih.gov/), China Glioma Genome Atlas (CGGA) Data Portal (http://www.cgga.org.cn/), and GSE0160011 (http//:www.ncbi.nlm.nih.gov/) were used to select differentially expressed lncRNA, miRNAs and target genes. Furthermore, we used StarbaseV2.0 (http://starbase.sysu.edu.cn) and lncRNASNP2 (http://bioinfo.life.hust.edu.cn/lncRNASNP/#!/) to predict the potentially targeting relationship between lncRNA and miRNAs. Based on the dual luciferase reporter assay results, lncRNASNP2 was used to predict the binding site between NETA1 and miR-324-5p. By using three online prediction tools Targetscan(http://www.targetscan.org/), miRDB(http://mirdb.org), (miRWalkhttp://mirwalk.umm.uni-heidelberg.de) to search for specific miRNA-mRNA relationships. The different results of online data prediction are analyzed and used to draw Venn diagrams (https://bioinfogp.cnb.csic.es/tools/venny/index.html). In addition, putative binding sites between miR-324-5p and KCTD20 from Targetscan were used for miRNA target validation analysis.

Statistical analysis

All statistical analyses were performed using Prism 7 software (La Jolla, CA, USA). All experiments were performed in triplicate with means and standard error of the mean or standard deviation subjected to the Student's t-test for pairwise comparison or ANOVA for multivariate analysis. Analysis of patient survival was performed using Kaplan-Meier analysis, and significance was determined by the log-rank test. Correlations between NEAT1, miR-324-5p, KCTD20 were analyzed by Spearman's rank correlation. A significance level set at $P<0.05$ was considered significant for all the tests.

Results

NEAT1 is identified as a highly overexpressed lncRNA and correlated with a poor prognosis in glioma cancer.

To evaluate the expression of glioma cancer-related lncRNAs that may be involved in tumorigenesis, we first analyzed data from the TCGA database. The results found that NEAT1 expression was significantly upregulated in high grade gliomas(HGG) compared to low grade gliomas (LGG) (Fig. 1A). In order to explore the role of NEAT1 in glioma, we first detected the relative expression levels of NEAT1 in 43 paired glioma tissues/adjacent noncancerous tissue specimens by quantitative reverse transcription PCR (qRT-PCR). As shown in Fig. 1B, an increase in NEAT1 expression was observed in glioma tissues compared to the corresponding adjacent normal tissues. In six glioma cell lines (U87, LN229, H4, U251, U118, A172), the expression of NEAT1 obviously elevated compared with normal cell line NHA (Fig. 1C), especially in U251 and LN229. In addition, using fluorescent in situ hybridization (FISH), we found that the glioma tissues exhibited significantly higher NEAT1 staining intensity compared with adjacent normal brain tissues (Fig. 1D). Immunohistochemistry (IHC) assays indicated that proliferation marker Ki-67 expression was lower in normal samples than the gliomas (Fig. 1D). We furtherly conducted Kaplan–Meier survival analysis using the data from the TCGA database, and found that patients with high-NEAT1 levels frequently had shorter overall survival time than those with low-NEAT1 (Fig. 1E). As presented in Table 1, a higher NEAT1 expression was observed more frequently in patients with larger tumor size ($P = 0.047$) and advanced WHO stage ($P = 0.024$). Taken together, these data suggest that NEAT1 expression is significantly upregulated in gliomas and could serve as a prognostic marker for glioma patients.

NEAT1 promotes the proliferation of glioma cells and inhibits apoptosis in vitro.

To explore the potential biological processes of NEAT1 involvement in glioma, we performed gain- and loss-of-function studies on the function cell proliferation and apoptosis through glioma cells. Based on the above analysis of NEAT1 expression in glioma cell lines (Fig. 1C), we selected U251 and LN229 cell lines for subsequent experiments. We silenced NEAT1 expression in U251 and LN229 cells by transfecting siNEAT1. At the same time, we transfected these two cell lines with pcDNA 3.1-NEAT1 expression vector to induce the ectopic overexpression of NEAT1. The qRT-PCR analysis was performed 48 h after transfection to detected its efficiency. The results indicated that knocking down of NEAT1 showed higher interference efficiency in both U251 and LN229 cell lines (Fig. 2A). And comparing with control groups, NEAT1 expression was remarkably higher in the pcDNA-NEAT1 groups than in the empty

vector groups (Fig. 2A). Then the cell proliferation of U251 and LN229 cells were monitored using CCK-8,EdU and colony formation assays. Firstly, we conducted the CCK-8 assay to evaluate the effect of NEAT1 on cell viability. As shown in Fig. 2B, cell proliferation curve showed that downregulation of NEAT1 significantly inhibited cell growth compared with the controls. In contrast, overexpression of NEAT1 promoted cell proliferation in both U251 and LN229 cells (Fig. 2C). Consistently, the colony formation assays showed the similar results (Fig. 2D-E). EdU incorporation experiments was carried out to further testify the proliferative ability of NEAT1. The data showed that silencing NEAT1 expression by siNEAT1 significantly suppressed the EdU-positive rate of in both U251 and LN229 cells, while ectopic expression of NEAT1 increased EdU-positive cells (Fig. 2F-G). As well, TUNEL assay showed that cell apoptosis rate was increased in siNEAT1 group compared with that in siCtrl group, while it is decreased in pcDNA-NEAT1 group compared with that in corresponding control groups (Fig. 2H-I). Collectively, these results suggested that NEAT1 may serve as an oncogene for glioma cells during cancer progression.

Knockdown of NEAT1 induces apoptosis and G1 arrest of glioma cells in vitro and glioma tumorigenesis in vivo.

Increased cell cycle arrest and apoptosis are two factors that may help clarify the research mechanism of cancer cell proliferation. Therefore, we examined differences in cell-cycle distributions following NEAT1 overexpression or silencing by flow cytometry analysis. Downregulation of NEAT1 resulted in a notable accumulation of cells in G0/G1 phase and a decrease in S-phase cells (Fig. 3A), whereas cell-cycle progression beyond the G1–S transition was observed in NEAT1-overexpression of U251 and LN229 cells (Fig. 3B). The results indicated that the proportion of apoptotic cells treated with siNEAT1 increased significantly, but decreased in the pcDNA-NEAT1 groups. (Fig. 3C-D). In addition, western blotting analysis showed that the expression levels of cell cycle-related proteins (CDK-4 and cyclin D1) and apoptosis-related proteins (Bcl-2, Bax) are highly consistent with their respective rates of apoptotic and percentage of cell cycle progression (Fig. 3E).

To examine the potential role of lncRNA NEAT1 in vivo, U251 cells transfected with shCtrl or shNEAT1 was intracranially injected into immunocompromised nude mice. At 7, 14, 21, and 28 days after implantation, compared with the blank control group, silencing of NEAT1 significantly inhibited the intracranial tumor growth (Fig. 3F) Meanwhile,these findings were further confirmed by the survival curves (Fig. 3G). Representative H&E staining shown in Fig. 3H, tumor volumes were significantly different between two groups. Compared to shCtrl tumors, immunohistochemical staining of Ki-67 showed reduced expression in shNEAT1 group (Fig. 3H). These data indicate that the inhibitory effect of NEAT1 silencing on glioma cell proliferation may be attributed to increased apoptosis and cell cycle arrest, and confirm the carcinogenic activity of NEAT1 on gliomas in vivo.

NEAT1 functions as a ceRNA by competitively binding miR-324-5p.

A potential mechanism for competitive RNA (ceRNA) has been proposed, and recent studies have shown that many lncRNAs function as ceRNA for specific miRNAs(30, 31), which increases the level of posttranscriptional regulation. Emerging evidence have shown that NEAT1 acts as ceRNA in various

cancers, including glioma(32), but lncRNAs may regulate multiple targets by functioning as ceRNA to adsorb more than one miRNA. To figure out the potential candidate miRNAs of NEAT1, we used online target prediction tools StarbaseV2.0 and lncRNASNP2, and thirteen miRNAs were chosen (Fig. 4A). Based on the glioma expression levels in the TCGA database, we found that four of the thirteen miRNAs selected had significantly lower expression in tumor compared to normal tissues (Fig. 4B, Fig. S1A). The CCGA database also showed that miR-324-5p expression was significantly reduced in high grade glioma (Fig. 4C). We further tested four miRNAs (miR-125a, miR-324-5p, miR-495-3p and miR-504) through dual luciferase reporter assays to confirm the interaction between NEAT1 and candidate miRNAs. The results show that miR-125a and miR-324-5p can inhibit luciferase activity, and miR-324-5p has a higher inhibitory efficiency (Fig. 4D). Therefore, we finally selected miR-324-5p for further research. To verify the direct binding relationship between NEAT1 and miR-324-5p (Fig. 4E), a wild type NEAT1 luciferase reporter vector (WT-NEAT1), and a mutant NEAT1 luciferase reporter vector (MUT-NEAT1) on predicted miR-324-5p binding sites of NEAT1 were constructed. As presented in Fig. 4F, we observed that miR-324-5p mimics reduced the luciferase activities of WT-NEAT1 transfection, compared with control group. To further validate the association relationship between NEAT1 and miR-324-5p, RNA immunoprecipitation (RIP) experiments was performed on U251 and LN229 cells transiently overexpressing miR-324-5p. The analysis showed that NEAT1 was highly enriched in cells transfected with miR-324-5p mimics compared to cells transfected with controls (Fig. 4G). The qRT-PCR data revealed that miR-324-5p levels was increased upon NEAT1 knockdown in both U251 and LN229 cells (Fig. 4H). However, ectopic expression of miR-324-5p had no effect on NEAT1 expression (Fig. S1B). Additionally, we evaluated the miR-324-5p expression in human glioma tissues and U251 and LN229 cell lines, as expected, miR-324-5p was significantly downregulated in both of them (Fig. 4I-J). Meanwhile, Spearman's correlation analysis demonstrated that there is a negative correlation between the expression of lncRNA NEAT1 and miR-324-5p in glioma samples (Fig. 4K). Taken together, these data demonstrated that NEAT1 associated with the miR-324-5p by functioning as a ceRNA.

Critical roles of miR-324-5p on glioma cell proliferation in vitro.

To examine whether miR-324-5p inhibits cell proliferation in glioma, we transfected U251 and LN229 cells with miR-324-5p inhibitor or miR-324-5p mimics (Fig. 5A, Fig. S1C). The CCK-8, colony formation, and EdU assays were performed and found that miR-324-5p inhibitor dramatically increased glioma cell proliferation and colony formation ability, while overexpressing of miR-324-5p could inhibit cells viability in both U251 and LN229 (Fig. 5B-D, Fig. S1D-E). Consistent with our expected results, TUNEL analysis showed that downregulated expression of miR-324-5p suppressed glioma cell apoptosis (Fig. 5E), while overexpression of miR-324-5p shows opposite results (Fig. S1F). Furthermore, data from the flow cytometry analysis showed that silencing of miR-324-5p decreased cell apoptosis and cell cycle arrest at G0/G1 phase (Fig. 5F-G); Inversely, more apoptotic cells and percentage of cells in G0/G1 phase were observed after cells were transfected with miR-324-5p mimics (Fig. S1G-H). Parallel western blotting experiments were performed in LN229/U251 cells, downregulation of miR-324-5p led to a significant decrease in Bax, and an increase in Bcl-2 and cell cycle-related proteins CDK4 and Cyclin D1 (Fig. 5H). As shown in Fig. S1I, the corresponding protein expression results also appeared in the mimics group.

Together, these results indicate a possible inhibitory role of miR-324-5p in the regulation of glioma progression.

Silencing of miR-324-5p reversed the suppressive effects on glioma cells induced by downregulation of NEAT1.

According to the above results, we noticed that the reduced proliferative capacity of NEAT1 knockdown was similar to those of miR-324-5p overexpression, suggesting that downregulation of NEAT1 might be a mechanism to reduce the tumorigenesis of glioma cells by regulating miR-324-5p expression. To confirm whether miR-324-5p is involved the NEAT1-regulated tumorigenesis, the combinations of transfection was performed before assessing glioma cell proliferation and apoptosis assays. As shown in Fig. 6A-C, these results showed that the inhibitory effects of siNEAT1-mediated could partially be rescued when U251 and LN229 cells were co-transfected with miR-324-5p inhibitor. The results of flow cytometry analysis showed that compared with the co-transfection groups, higher rate of cell cycle arrest and apoptosis were observed in siNEAT1 group while the miR-324-5p inhibitor group showed lower rates (Fig. 6D-F). Analysis of the above co-transfected cells in Western blot experiments also showed the same results (Fig. 6G). Our results showed that siNEAT1 inhibited the proliferation of glioma cells and induce cell cycle arrest and apoptosis, while miR-324-5p downregulation could partially eliminate these regulatory effects.

NEAT1 positively regulates KCTD20 expression through competing with miR-324-5p.

To further clarify the ceRNA regulation mechanism by which NEAT1/miR-324-5p regulates glioma cell proliferation, we used online informatics tools TargetScan, miRDB and miRWalk to predict the downstream target genes that involved in NEAT1 competitive binding to miR-324-5p. As illustrated in Fig. 7A, there are 52 target genes with potential binding sites for miR-324-5p. Among them, we found that six genes in the TCGA database had significantly higher expression in glioma tissues compared to normal tissues ($P < 0.05$) (Fig. S2A-B). To select the most effective target gene associated with miR-324-5p, U251 and LN229 cells were transfected with a construct containing a suppressor or negative control for miR-324-5p. Immunoblotting and qRT-PCR results revealed that compared with the expression levels of the other five genes, the expression levels of KCTD20 was significantly increased at the protein level and mRNA level when miR-324-5p was downregulated (Fig. 7B). We further detected the expression of KCTD20 in glioma tissues and showed that it was consistent with TCGA, CGGA and GSE10611 database results (Fig. 2C, Fig. S2B). As presented in Fig. 7D, the miRNA: mRNA alignment analysis showed that the 3 ' UTR of KCTD20 contains one putative binding site for miR-324-5p. A significant repression of luciferase activity upon miR-324-5p transfection was observed in both U251 and LN229 cells when wild-type KCTD20 plasmids was present (Fig. 7E), indicating that miR-324-5p binds to KCTD20 in a sequence-specific manner. Therefore, we further analyzed the regulatory relationship between KCTD20 and miR-324-5p in glioma cells. The protein and mRNA expression levels of KCTD20 in U251 and LN229 cells was evaluated or decreased after being transfected with miR-324-5p inhibitor or miR-324-5p mimics (Fig. 7F). We have preliminary demonstrated that miR-324-5p downregulation can partially reverse the inhibitory

effects of silencing NEAT1, and miR-324-5p can regulate the expression of KCTD20. Therefore, we continue to study the association between NEAT1 and KCTD20. As exhibited in Fig. 7G, KCTD20 levels was dramatically reduced after NEAT1 knockdown in the 2 glioma cell lines. However, silencing of miR-324-5p could markedly abolished the inhibitory effects of siNEAT1 both in KCTD20 mRNA and protein levels (Fig. 7H). As expected, IHC experiment showed lower KCTD20 expression in shNEAT1 mouse xenograft tumors than control groups (Fig. S2C). Furtherly, we analyzed the correlation between NEAT1 and KCTD20 expression levels in glioma cancer tissues. As presented in Fig. 7I, the result displayed that KCTD20 was positively correlated with NEAT1 in glioma tissues, consistent with the potential regulatory axis of NEAT1/miR-324-5p/KCTD20 pathway. These data, taken together, suggested that lncRNA NEAT1 may regulates the expression of KCTD20 through post-transcriptional modulation of miR-324-5p.

KCTD20 is involved in NEAT1-induced tumor proliferative capability in vitro and in vivo.

In order to elucidate the carcinogenic effect of KCTD20 in gliomas, we first evaluated its expression in gliomas and normal tissues. Analysis of KCTD20 expression using the TCGA, CGGA and GSE10611 database revealed that KCTD20 was significantly upregulated in tumor samples compared to normal samples (Fig. S2B). Similarly, IHC staining of glioma samples showed that NEAT1 protein abundance is increased in glioma tissues (Fig. S2C). In order to verify the role of KCTD20 in the proliferation of glioma cells, U251 and LN229 cells were transfected with siKCTD20 or negative control plasmids for western blot and qRT-PCR experiments (Fig. 8A). CCK-8 and colony formation assays showed that silencing of KCTD20 inhibited the proliferative viability of human glioma cells in vitro, and EdU incorporation analysis also showed the similar result (Fig. 8B-D). Next, we performed the flow cytometry analysis. The data suggested that cells transfected with siKCTD20 increased cell cycle arrest and had higher apoptotic rate in comparison with controls (Fig. S3A-B). In cells that suppressed KCTD20 expression, we found that CyclinD1, CDK4, and Bcl-2 protein levels were reduced, while Bax protein levels were increased (Fig. S3C). To examine the role of KCTD20 on glioma cell proliferation, U251 cells were transfected with lentiviral constructs containing shRNA against KCTD20 (shKCTD20) or the negative control (shNC) and injected into mouse brains. We found that KCTD20 silencing could notably inhibit glioma cell tumor growth in vivo (Fig. S3D-F). In addition, cell proliferation and apoptosis assays presented that knockdown of the miR-324-5p stimulated the proliferation and inhibited apoptosis of U251 and LN229 cells, and this cancer-promoting effect was partially reversed after the downregulation of KCTD20 by siKCTD20 (Fig. 8E-G, Fig. S2H). Moreover, as shown in Fig. 8H-K, concomitant suppression of miR-324-5p and KCTD20 abrogated the effect of KCTD20 knockdown on the cell apoptosis and reversed the siKCTD20-induced G1 arrest of U251 and LN229 cells compared with cells transfected with siKCTD20 and the control groups. And the transfection of miR-324-5p inhibitor increased the KCTD20 expression at both mRNA and protein levels, while the simultaneous upregulation of KCTD20 restored to a relatively normal level after co-transfection with siKCTD20(Fig. 8L, S3G). Furthermore, the reduced CDK4, Cyclin D1 and Bcl-2 expression in siKCTD20 group was rescued by inhibition of miR-324-5p, and Bax expression is consistent with the above results (Fig. 8L). A statistically significant inverse correlation was observed between miR-324-5p and KCTD20 expression levels in 43 glioma specimens ($r = -0.4582$, $P = 0.002$, Fig. S3I). Taken together,

these data provide substantial evidence that NEAT1 could promote glioma cell proliferation and exert oncogenic functions by modulating miR-324-5p/KCTD20.

Discussion

Over the past decades, tremendous efforts have been made to identify cancer-related lncRNAs and elucidate their biological role in development and progression of numerous human diseases, including cancers(33–35). Currently, lncRNAs has been accepted as important regulatory factors in cancer progression and different biological processes such as chromatin remodeling, transcriptional and posttranscriptional regulation(36). Although a large number of lncRNAs have been annotated(37), functional interpretation has only just begun. Studies show that 18% of these lncRNAs are related to human tumors, while human protein-coding genes account for only 9% (38). Therefore, more lncRNAs related to gliomas and a more systematic study of the molecular mechanisms of glioma progression need to be explored. Eventually it will become an important part of the early diagnosis and treatment of glioma, and it will help clinicians to evaluate the prognosis of glioma patients.

LncRNA NEAT1 has been reported to be upregulated in numerous tumor samples and identified as a potential therapeutic target for many cancers(39). According to Shin et al.'study, NEAT1 is regarded as an oncogenic factor in breast cancer, and downregulation of NEAT1 suppresses the proliferation of breast cancer cell(40). Herein, we found that NEAT1 was overexpressed in glioma specimens and cell lines and mediated miR-324-5p/KCTD20. In addition, silencing NEAT1 could significantly inhibit cell viability, further affect cell propagation and induce cell apoptosis capacities in glioma. Furthermore, knockdown of miR-324-5p in glioma cells demonstrated the opposite results. All these data indicated our conclusion that ectopic expression lncRNA NEAT1 may represent a poor prognostic indicator in glioma and may become a potential therapeutic strategy for the treatment of patients with gliomas.

Recently, a growing number of studies have reported that a new regulatory mechanism involving ceRNAs between lncRNAs and miRNAs, where lncRNAs could modulate related RNAs by binding and titrating them off their binding sites on protein-coding messengers(41, 42). LncRNAs might function as a ceRNA or a molecular sponge in modulating miRNAs, by which lncRNAs can sponge miRNAs to block the tumor suppressor role of specific miRNAs and release the suppression effects of oncogenes caused by miRNAs to facilitate tumor initiation. For example, lncRNA PSMA3-AS1 has been found to act as a ceRNA to promote esophageal cancer cell progression and the expression of proto-oncogene EZH2 through negative modulation of miR-101(43). LncRNA UCA1 functioned as an endogenous sponge ofmiR-182-5p to positively regulate the expression of Delta-like ligand 4(DLL4) in renal cancer cells(44). In addition, some studies have confirmed that NEAT1 can play a regulatory role through competitively binding different miRNAs in a variety of cancers(45, 46). These studies have uncovered a new way to elucidate regulatory mechanisms between NEAT1 and KCTD20. Therefore, we performed the bioinformatics analysis and found thirteen miRNAs that could bind to complementary sequences in NEAT1. Next, we confirmed that miR-324-5p can bind to NEAT1 by luciferase reporter assays and RIP analysis. Combined with the online bioinformatics prediction and the predicted expression level from TCGA database, miR-

324-5p was finally selected as a candidate gene that NEAT1 can bind. By applying the methods of loss- and gain-of-function, we demonstrated that NEAT1 plays a role in cell proliferation, cell cycle processes and cell apoptosis in glioma. These results revealed that NEAT1 exerts physiological functions via directly binding to miR-324-5p. Interestingly, recent research reported that lncRNA can function as ceRNA and interfere with miRNAs, and ultimately exert its regulatory effect on mRNAs at the post-transcriptional level(47, 48). In this study, we further verified that lncRNAs can regulate mRNAs post-transcription in glioma cells by acting as ceRNA in combination with miRNAs. Our data revealed that NEAT1 reverses the effects of miR-324-5p on glioma cell proliferation, cell cycle and apoptosis through post-transcriptional regulation of KCTD20 expression levels.

KCTD20 (potassium channel tetramerization protein domain containing 20), located in chromosome 6, is a newly identified protein which is an isoform of BTBD10 (BTB domain-containing protein 10) and harbors a C-terminal amino-acid sequences similar to BTBD10(49). Some reports have identified that KCTD family proteins may be involved in regulating cell proliferation(50). Studies have shown that KCTD20 is an oncogene that can promote the development of small cell lung cancer by activating the Fak/AKT pathway(51). But the role of KCTD20 in tumorigenesis and development is still unclear, especially in glioma. To investigate whether NEAT1-induced miR-324-5p inhibition led to the overexpression of its target mRNA and promote the occurrence and progression of glioma, we further studied the miR-324-5p target gene KCTD20. We explored the association between miR-324-5p and KCTD20 through bioinformatics analysis, and found that the protein expression level of KCTD20 can be suppressed by miR-324-5p. The luciferase reporter vector assays were analyzed, suggesting that miR-324-5p inhibits KCTD20 levels by directly binding to its 3’-UTR. Furthermore, we investigated whether KCTD20 can promote tumor growth via loss-of-function assays. Our data firstly showed that knockdown of KCTD20 inhibited glioma cell proliferation, as well as promoted the apoptosis and induced G0/G1 cell cycle arrest, indicating the tumorigenic activity of KCTD20 in glioma. In addition, Spearman's correlation analysis indicated that miR-324-5p were inversely correlated with NEAT1 and KCTD20 expression, while there has a positive correlation between NEAT1 and KCTD20. These findings are consistent with our results, which also reveal new mechanisms for regulating KCTD20 expression.

In conclusion, our current experimental results provide mechanistic insights, highlighting that lncRNA NEAT1 could act as a molecular sponge of miR-324-5p and significantly contributed to the occurrence and progression of glioma by activating KCTD20 protein expression. Shedding new light on the potential understanding of the molecular network of glioma cancer progression. Taken together, our findings suggest that lncRNA NEAT1 may be used as a prognostic factor for glioma patients, and it can also be considered as a potential biomarker and target for glioma cancer treatment.

Declarations

Acknowledgements

We thank all the contributors for this work.

Authors' contributions

WPL and XML designed the study. JLZ, YYL and YQL performed the experiments and collected the data. GZX, YH carried out data analyses. JLZ and YYL prepared the manuscript draft. WPL and XML revised the manuscript. All authors read and approved the final manuscript.

Funding

This research was supported by Natural Science Foundation of China (No.81627806). Six Talent Peaks Project in Jiangsu Province (Six Talent Peaks Project in Jiangsu Province of China) - [2015-WSN- 023 (IB15)].

Corresponding author

Weiping Liu, Department of Neurosurgery, Xijing Hospital, Fourth Military Medical University, No.17 Changle West Road, Xi'an 710032, Shannxi Province, People's Republic of China. E-mail: neurosurgeonliu@163.com

Xiaoming Lu, Department of Neurosurgery, The First Affiliated Hospital of Nanjing Medical University, Nanjing 210029, Jiangsu Province, People's Republic of China. E-mail: luxm923@126.com

Availability of data and materials

All data and material are available from the corresponding author.

Ethics approval and consent to participate

This research was reviewed and approved by the Ethics Committee the Fourth Military Medical University and the First Affiliated Hospital of Nanjing Medical University.

Consent for publication

The publication of this manuscript has been approved by all authors.

Disclosure of conflict of interest

The authors declare that they have no conflict of interest.

References

1. Ricard D, Idbaih A, Ducray F, Lahutte M, Hoangxuan K, Delattre JY. Primary brain tumours in adults. 2012;379(9830):1984–96.
2. Weller M, Cloughesy T, Perry JR, Wick W. Standards of care for treatment of recurrent glioblastoma–are we there yet? Neurooncology. 2013;15(1):4–27.

3. Wang J, Su HK, Zhao HF, Chen ZP, To SS. Progress in the application of molecular biomarkers in gliomas. Biochem Biophys Res Commun. 2015;465(1):1–4.
4. Stupp R, Mason WP, van den Bent MJ, Weller M, Fisher B, Taphoorn MJ, et al. Radiotherapy plus concomitant and adjuvant temozolomide for glioblastoma. N Engl J Med. 2005;352(10):987–96.
5. Shi X, Sun M, Liu H, Yao Y, Song Y. Long non-coding RNAs: a new frontier in the study of human diseases. Cancer letters. 2013;339(2):159–66.
6. Ponting CP, Oliver PL, Reik W. Evolution and functions of long noncoding RNAs. Cell. 2009;136(4):629–41.
7. Sheik Mohamed J, Gaughwin PM, Lim B, Robson P, Lipovich L. Conserved long noncoding RNAs transcriptionally regulated by Oct4 and Nanog modulate pluripotency in mouse embryonic stem cells. RNA (New York). 2010;16(2):pp. 324–37.
8. Yang L, Froberg JE, Lee JT. Long noncoding RNAs: fresh perspectives into the RNA world. Trends Biochem Sci. 2014;39(1):35–43.
9. Guttman M, Donaghey J, Carey BW, Garber M, Grenier JK, Munson G, et al. lincRNAs act in the circuitry controlling pluripotency and differentiation. Nature. 2011;477(7364):295–300.
10. Bueno MJ, Perez de Castro I, Malumbres M. Control of cell proliferation pathways by microRNAs. Cell cycle (Georgetown Tex). 2008;7(20):3143–8.
11. Cesana M, Cacchiarelli D, Legnini I, Santini T, Sthandier O, Chinappi M, et al. A long noncoding RNA controls muscle differentiation by functioning as a competing endogenous RNA. Cell. 2011;147(2):358–69.
12. Tsai MC, Manor O, Wan Y, Mosammaparast N, Wang JK, Lan F, et al. Long noncoding RNA as modular scaffold of histone modification complexes. Science. 2010;329(5992):689–93.
13. Cai B, Zheng Y, Ma S, Xing Q, Wang X, Yang B, et al. Long noncoding RNA regulates hair follicle stem cell proliferation and differentiation through PI3K/AKT signal pathway. Mol Med Rep. 2018;17(4):5477–83.
14. Zheng W, Yu A. EZH2-mediated suppression of lncRNA-LET promotes cell apoptosis and inhibits the proliferation of post-burn skin fibroblasts. Int J Mol Med. 2018;41(4):1949–57.
15. Zheng P, Yin Z, Wu Y, Xu Y, Luo Y, Zhang TC. LncRNA HOTAIR promotes cell migration and invasion by regulating MKL1 via inhibition miR206 expression in HeLa cells. Cell communication signaling: CCS. 2018;16(1):5.
16. Cech TR, Steitz JA. The noncoding RNA revolution-trashing old rules to forge new ones. Cell. 2014;157(1):77–94.
17. Salmena L, Poliseno L, Tay Y, Kats L, Pandolfi PP. A ceRNA hypothesis: the Rosetta Stone of a hidden RNA. language? Cell. 2011;146(3):353–8.
18. Zhang G, Li S, Lu J, Ge Y, Wang Q, Ma G, et al. LncRNA MT1JP functions as a ceRNA in regulating FBXW7 through competitively binding to miR-92a-3p in gastric cancer. Mol Cancer. 2018;17(1):87.

19. Zhao L, Zhou Y, Zhao Y, Li Q, Zhou J, Mao Y. Long non-coding RNA TUSC8 inhibits breast cancer growth and metastasis via miR-190b-5p/MYLIP axis. Aging. 2020;12(3):2974–91.
20. Clemson CM, Hutchinson JN, Sara SA, Ensminger AW, Fox AH, Chess A, et al. An architectural role for a nuclear noncoding RNA: NEAT1 RNA is essential for the structure of paraspeckles. Molecular cell. 2009;33(6):717–26.
21. Chakravarty D, Sboner A, Nair SS, Giannopoulou E, Li R, Hennig S, et al. The oestrogen receptor alpha-regulated lncRNA NEAT1 is a critical modulator of prostate cancer. Nature communications. 2014;5:5383.
22. Dong P, Xiong Y, Yue J, Xu D, Ihira K, Konno Y, et al. Long noncoding RNA NEAT1 drives aggressive endometrial cancer progression via miR-361-regulated networks involving STAT3 and tumor microenvironment-related genes. Journal of experimental clinical cancer research: CR. 2019;38(1):295.
23. Dong P, Xiong Y, Yue J, Hanley SJB, Kobayashi N, Todo Y, et al. Long Non-coding RNA NEAT1: A Novel Target for Diagnosis and Therapy in Human Tumors. Frontiers in genetics. 2018;9:471.
24. Kong X, Zhao Y, Li X, Tao Z, Hou M, Ma H. Overexpression of HIF-2alpha-Dependent NEAT1 Promotes the Progression of Non-Small Cell Lung Cancer through miR-101-3p/SOX9/Wnt/beta-Catenin Signal Pathway. Cellular physiology and biochemistry: international journal of experimental cellular physiology, biochemistry, and pharmacology. 2019;52(3):368–81.
25. Huang B, Liu C, Wu Q, Zhang J, Min Q, Sheng T, et al. Long non-coding RNA NEAT1 facilitates pancreatic cancer progression through negative modulation of miR-506-3p. Biochem Biophys Res Commun. 2017;482(4):828–34.
26. C P, Z C. S W, HW W, W Q, L Z, et al. The Error-Prone DNA Polymerase κ Promotes Temozolomide Resistance in Glioblastoma through Rad17-Dependent Activation of ATR-Chk1 Signaling. 2016;76(8):2340–53.
27. Zhang R, Luo H, Wang S, Chen W, Chen Z, Wang HW, et al. MicroRNA-377 inhibited proliferation and invasion of human glioblastoma cells by directly targeting specificity protein 1. Neurooncology. 2014;16(11):1510–22.
28. Fan L, Chen Z, Wu X, Cai X, Feng S, Lu J, et al. Ubiquitin-Specific Protease 3 Promotes Glioblastoma Cell Invasion and Epithelial-Mesenchymal Transition via Stabilizing Snail. Molecular cancer research: MCR. 2019;17(10):1975–84.
29. Chen Z, Wang HW, Wang S, Fan L, Feng S, Cai X, et al. USP9X deubiquitinates ALDH1A3 and maintains mesenchymal identity in glioblastoma stem cells. J Clin Investig. 2019;129(5):2043–55.
30. Cao C, Sun J, Zhang D, Guo X, Xie L, Li X, et al. The long intergenic noncoding RNA UFC1, a target of MicroRNA 34a, interacts with the mRNA stabilizing protein HuR to increase levels of beta-catenin in HCC cells. Gastroenterology. 2015;148(2):415 – 26.e18.
31. Guil S, Esteller M. RNA-RNA interactions in gene regulation: the coding and noncoding players. Trends Biochem Sci. 2015;40(5):248–56.

32. Zhou K, Zhang C, Yao H, Zhang X, Zhou Y, Che Y, et al. Knockdown of long non-coding RNA NEAT1 inhibits glioma cell migration and invasion via modulation of SOX2 targeted by miR-132. Mol Cancer. 2018;17(1):105.
33. Gutschner T, Diederichs S. The hallmarks of cancer: a long non-coding RNA point of view. RNA Biol. 2012;9(6):703–19.
34. Gibb EA, Brown CJ, Lam WL. The functional role of long non-coding RNA in human carcinomas. Mol Cancer. 2011;10:38.
35. Feng Y, Hu X, Zhang Y, Zhang D, Li C, Zhang L. Methods for the study of long noncoding RNA in cancer cell signaling. Methods Mol Biol. 2014;1165:115–43.
36. Rinn JL, Chang HY. Genome regulation by long noncoding RNAs. Annual review of biochemistry. 2012;81:145–66.
37. Xie C, Yuan J, Li H, Li M, Zhao G, Bu D, et al. NONCODEv4: exploring the world of long non-coding RNA genes. Nucleic acids research. 2014;42(Database issue):D98–103.
38. Khachane AN, Harrison PM. Mining mammalian transcript data for functional long non-coding RNAs. PloS one. 2010;5(4):e10316.
39. Yu X, Li Z, Zheng H, Chan MT, Wu WK. NEAT1: A novel cancer-related long non-coding RNA. Cell Prolif. 2017;50(2).
40. Shin VY, Chen J, Cheuk IW-Y, Siu M-T, Ho C-W, Wang X, et al. Long non-coding RNA NEAT1 confers oncogenic role in triple-negative breast cancer through modulating chemoresistance and cancer stemness. Cell death disease. 2019;10(4):270-.
41. Yang C, Wu D, Gao L, Liu X, Jin Y, Wang D, et al. Competing endogenous RNA networks in human cancer: hypothesis, validation, and perspectives. Oncotarget. 2016;7(12):13479–90.
42. Jalali S, Bhartiya D, Lalwani MK, Sivasubbu S, Scaria V. Systematic transcriptome wide analysis of lncRNA-miRNA interactions. PloS one. 2013;8(2):e53823-e.
43. Qiu BQ, Lin XH, Ye XD, Huang W, Pei X, Xiong D, et al. Long non-coding RNA PSMA3-AS1 promotes malignant phenotypes of esophageal cancer by modulating the miR-101/EZH2 axis as a ceRNA. Aging. 2020;12(2):1843–56.
44. Wang W, Hu W, Wang Y, An Y, Song L, Shang P, et al. Long non-coding RNA UCA1 promotes malignant phenotypes of renal cancer cells by modulating the miR-182-5p/DLL4 axis as a ceRNA. Mol Cancer. 2020;19(1):18.
45. Wen J, Wang H, Dong T, Gan P, Fang H, Wu S, et al. STAT3-induced upregulation of lncRNA ABHD11-AS1 promotes tumour progression in papillary thyroid carcinoma by regulating miR-1301-3p/STAT3 axis and PI3K/AKT signalling pathway. Cell Prolif. 2019;52(2):e12569.
46. Li Y, Ding X, Xiu S, Du G, Liu Y. LncRNA NEAT1 Promotes Proliferation, Migration And Invasion Via Regulating miR-296-5p/CNN2 Axis In Hepatocellular Carcinoma Cells. OncoTargets therapy. 2019;12:9887–97.

47. Zhou M, Wang X, Shi H, Cheng L, Wang Z, Zhao H, et al. Characterization of long non-coding RNA-associated ceRNA network to reveal potential prognostic lncRNA biomarkers in human ovarian cancer. Oncotarget. 2016;7(11):12598–611.
48. Pang W, Lian F-Z, Leng X, Wang S-M, Li Y-B, Wang Z-Y, et al. Microarray expression profiling and co-expression network analysis of circulating LncRNAs and mRNAs associated with neurotoxicity induced by BPA. Environ Sci Pollut Res Int. 2018;25(15):15006–18.
49. Nawa M, Matsuoka M. KCTD20, a relative of BTBD10, is a positive regulator of Akt. BMC Biochem. 2013;14:27-.
50. Skoblov M, Marakhonov A, Marakasova E, Guskova A, Chandhoke V, Birerdinc A, et al. Protein partners of KCTD proteins provide insights about their functional roles in cell differentiation and vertebrate development. BioEssays: news reviews in molecular cellular developmental biology. 2013;35(7):586–96.
51. Zhang X, Zhou H, Cai L, Fan C, Liu Y, Wang L, et al. Kctd20 promotes the development of non-small cell lung cancer through activating Fak/AKT pathway and predicts poor overall survival of patients. Mol Carcinog. 2017;56(9):2058–65.

Tables

Table 1. Correlation of the expression of NEAT1 and glioma clinicopathologic features characteristics in 43 patients.

		NEAT1 expression levels		
Characteristics	**Number**	**Low expression**	**High expression**	***P* value**
Age(year)				
<45	19	9	10	0.658
≥45	24	13	11	
Gender				
Male	23	11	12	0.425
Female	20	12	8	
Tumor size				
<5 cm	25	16	9	**0.047***
≥5 cm	18	6	12	
Peritumoral brain edema				
<1 cm	22	9	13	0.287
≥1 cm	21	12	9	
WHO grade				
I-II	27	18	9	**0.024***
III-IV	16	5	11	

*$P < 0.05$ was considered significant

Figures

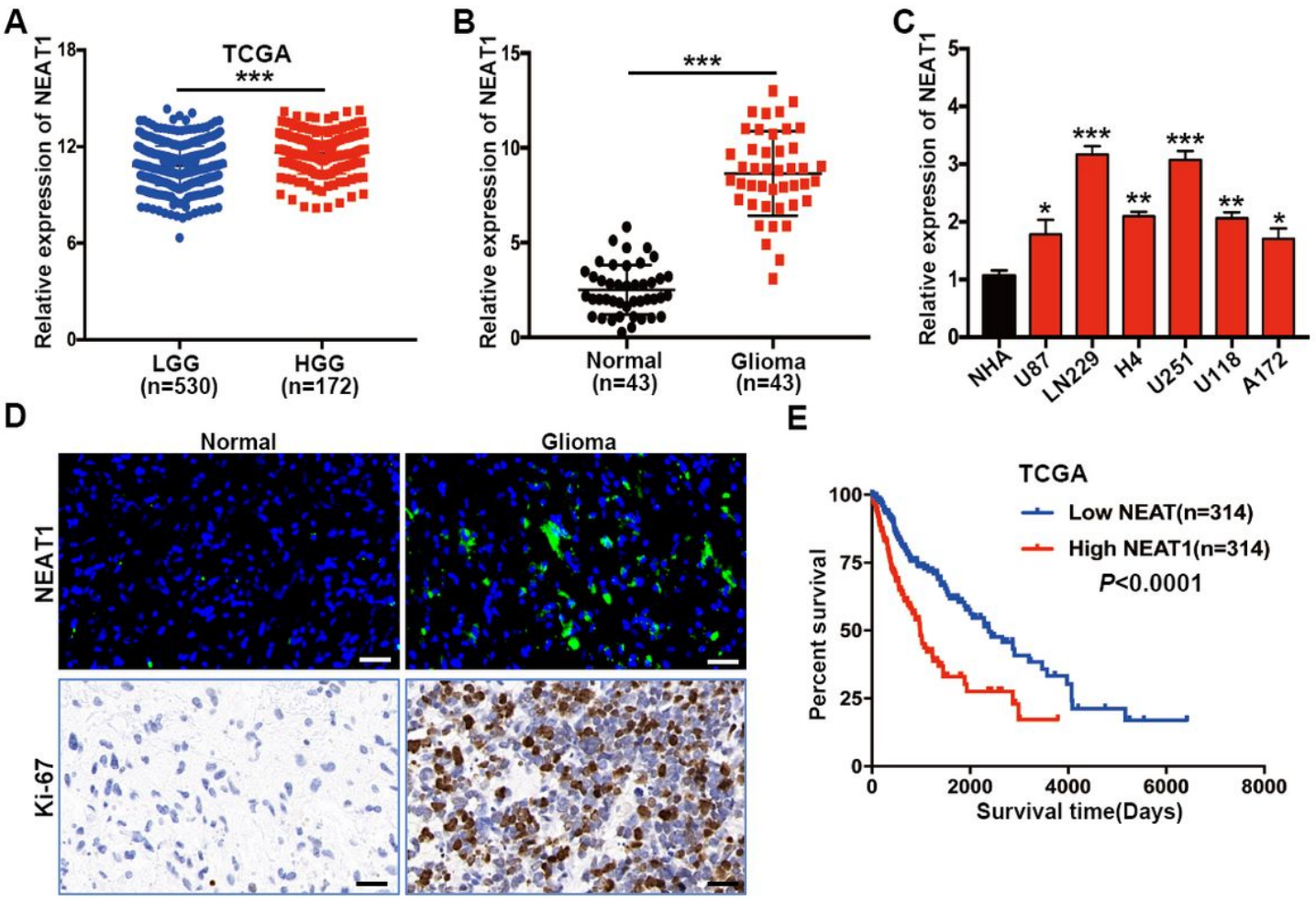

Figure 1

Expression levels of lncRNA NEAT1 in glioma samples and cell lines. A. The TCGA database showing increased NEAT1 expression in high-grade glioma tissues compared with that in low-grade glioma tissues. B. qRT-PCR analysis of NEAT1 expression in in 43 pairs of glioma tissues and adjacent non-tumor tissues and normalized against GAPDH expression. C. The expression of NEAT1 was detected by using qRT-PCR in normal human astrocytes (NHA), 6 glioma cells (U87, LN229, H4, U251, U118 and A172). D. Upper: The expression levels of NEAT1 in glioma tissues and their corresponding adjacent non-tumorous specimens was assessed by fluorescence in situ hybridization (FISH). scale bar=100μm; Lower: The expression levels of Ki-67 in normal and glioma tissues were assessed by IHC. scale bar=100μm E. Kaplan-Meier analysis was performed on glioma patients with high (n=314) or low (n=314) NEAT1 expression using the TCGA database (P<0.001). Values are shown as the mean ± standard errors of the mean based on three independent experiments. *P < 0.05, **P < 0.01, ***P < 0.001

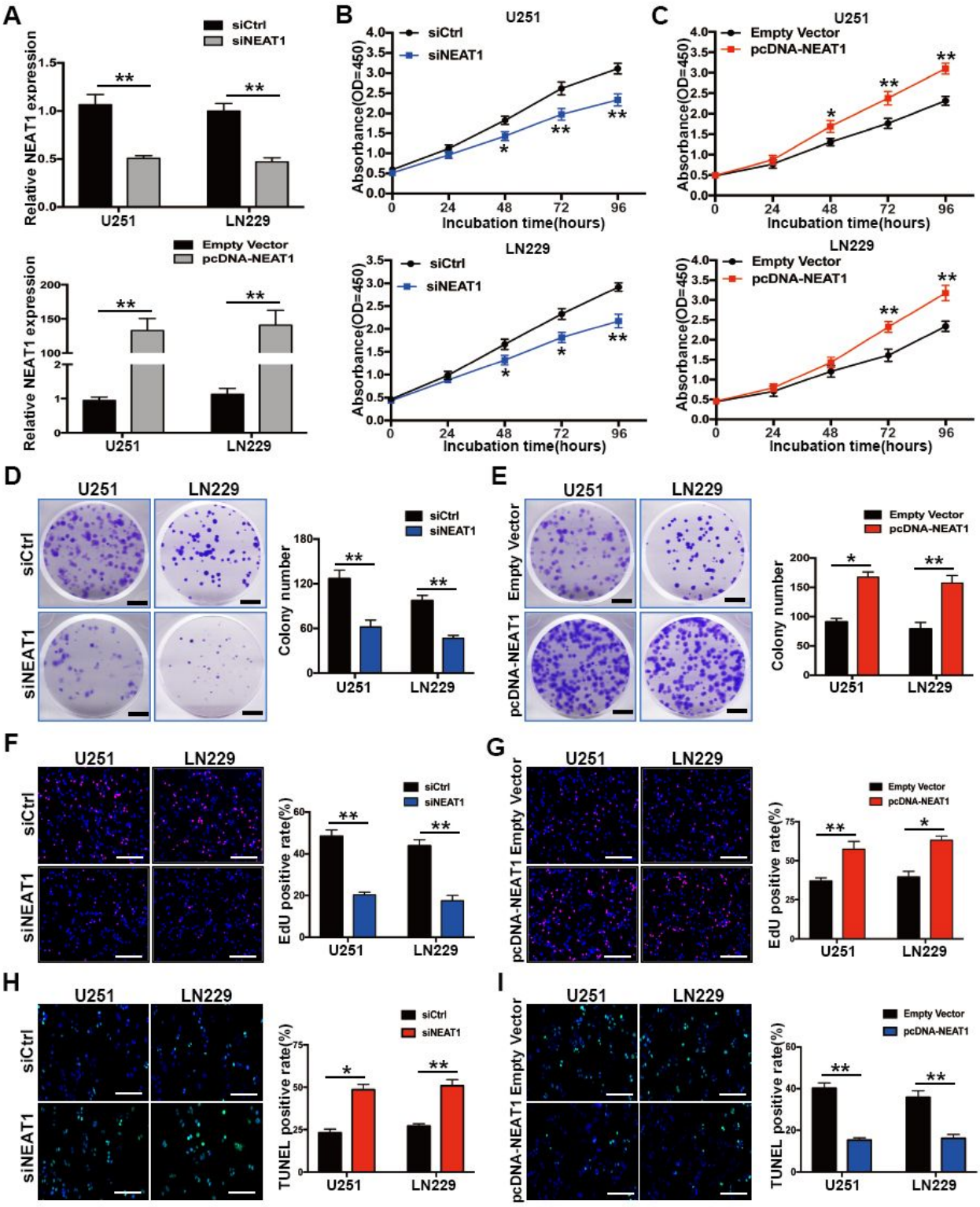

Figure 2

The role of lncRNA NEAT1 in glioma cell proliferation and apoptosis in vitro. A. siCtrl/siNEAT1 or Empty Vecotr/ pcDNA-NEAT1 was transfected into U251 and LN229 cells. The expression of NEAT1 was verified using qRT-PCR assays. B-C. Cell proliferation rates was determined in response to NEAT1 knockdown or overexpression using CCK-8 assays. D-E. Colony formation assays were performed to detect the proliferation of siNEAT1-transfected and pcDNA-NEAT1-transfected in both U251 and LN229 cells.

Colonies were counted and captured. scale bar=100μm. F-G. EdU staining assays were used to evaluate the growth in U251 and LN229 cells transfected with siNEAT1/pcDNA-NEAT1. scale bar=100μm. H-I. The TUNEL assay was used to detect the apoptosis of U251 and LN229 cells by silencing or overexpressing NEAT1. scale bar=100μm. Values are shown as the mean ± standard errors of the mean based on three independent experiments. *P < 0.05, **P < 0.01

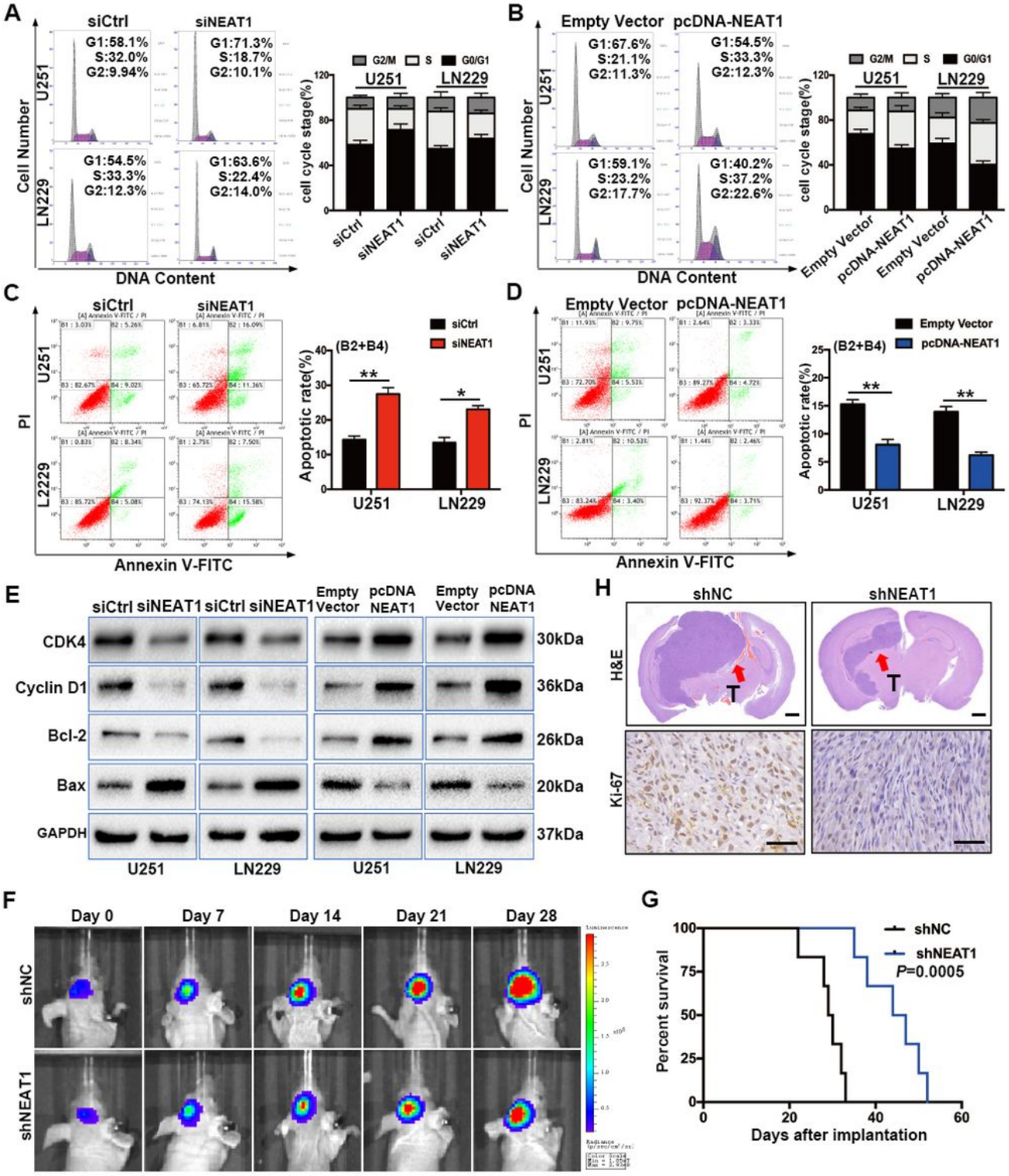

Figure 3

Effects of lncRNA NEAT1 on glioma cells apoptosis and cell cycle in vitro and in vivo. A-B. The cell cycle distribution of U251 and LN229 cells transfected with siNEAT1 or pcDNA-NEAT1 and corresponding negative controls. C-D. FACS analysis was performed to assess the apoptotic rates (B2+B4) of U251 and LN229 cells transduced with siCtrl and siNEAT1, or Empty Vector and pcDNA-NEAT1. B2, terminal apoptotic cells; B4, early apoptotic cells. E. Western blot analysis of the expression of cell cycle proteins (CDK4 and Cyclin D1) and cell apoptosis proteins (Bcl-2 and Bax) in both transfected U251 and LN229 cells. GAPDH was used as the loading control. F. The shNC-transfected and shNEAT1-transfected U251 cells were transplanted into orthotopic nude mice model respectively (n=6), and tumor formation was assessed by bioluminescence imaging. G. Survival curve of mice injected intracranially with shNC-infected U251 cells or shNEAT1-infected U251 cells. H. Representative H&E staining for tumor cytostructure and histological analysis to detect Ki-67 expression in tumors originated from shNC and shNEAT1-infected U251 cells. scale bar=1mm (upper panels) and 100μm (lower panels). Values are shown as the mean ± standard errors of the mean based on three independent experiments. *P < 0.05, **P < 0.01

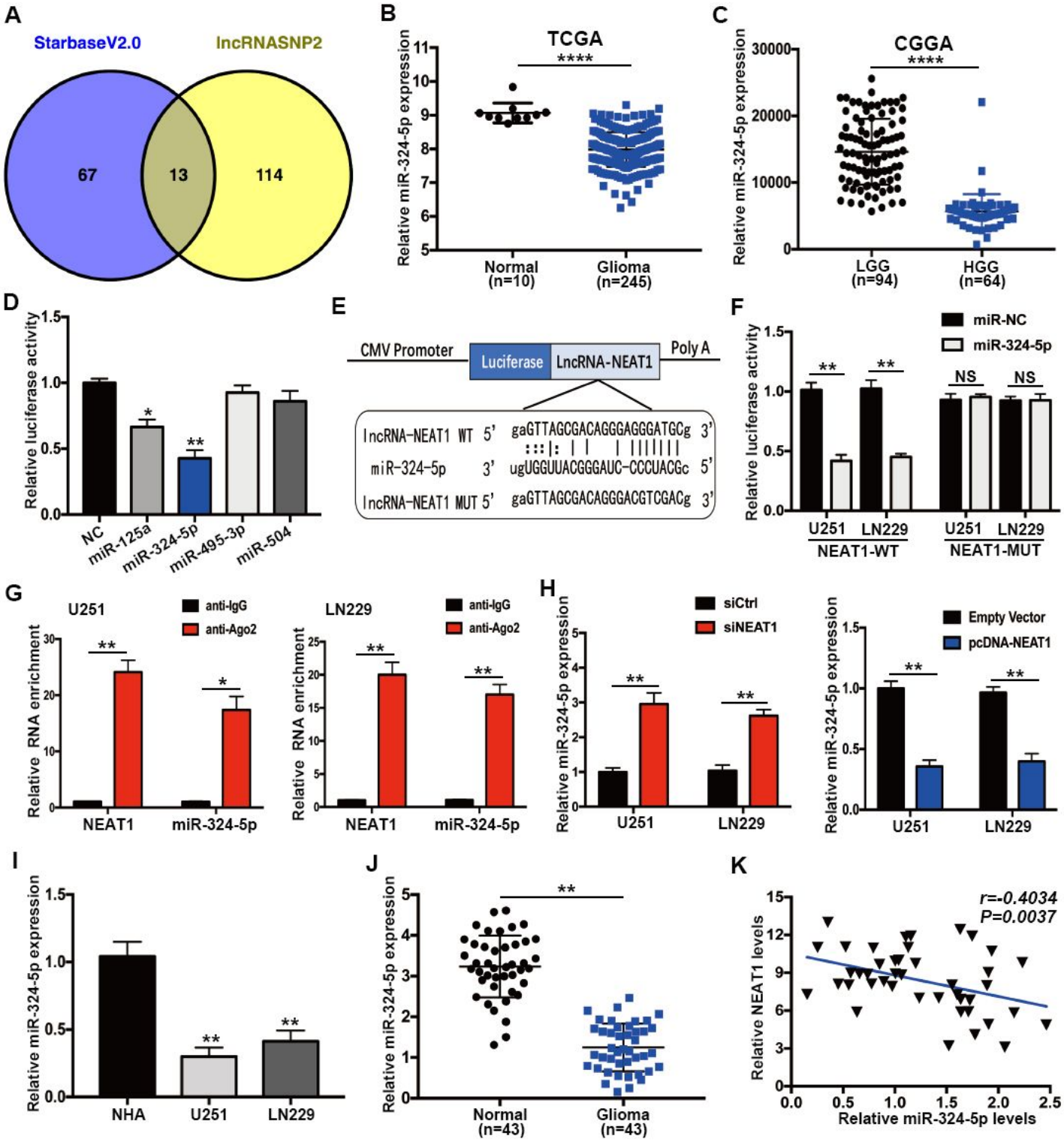

Figure 4

LncRNA NEAT1 directly interacted with miR-324-5p. A. Venn diagram displaying potential targets of NEAT1 by online prediction algorithms: Starbase V2.0 and lncRNASNP2. B-C. Relative expression of miR-324-5p in glioma tissues compared with normal tissues was analyzed by TCGA and CGGA database. D. The luciferase reporter plasmid containing NEAT1 sequence was respectively transfected with the four miRNA-coding plasmids into HEK-293T cells. E. The putative binding sequences of NEAT1 and miR-324-

5p, as predicted by lncRNASNP2. F. Luciferase activity in U251 and LN229 cells co-transfected with miR-324-5p mimics and luciferase reporter plasmid containing wild-type NEAT1 (NEAT1-WT) or mutant NEAT1 (NEAT1-MUT). G. RIP assays were applied to verify the interaction between NEAT1 and miR-324-5p, followed by qRT-PCR to analyze the expression levels of NEAT1 and miR-324-5p in Ago2 or IgG complexes. H. qRT-PCR was performed to examine miR-324-5p expression in U251 and LN229 cells transfected with siCtrl, siNEAT1, Empty Vector or pcDNA-NEAT1. I-J. The expression levels of miR-324-5p in glioma cell lines (U251 and LN229) and glioma tissues. K. Spearman's rank correlation analysis between NEAT1 and miR-324-5p levels in 43 paired glioma specimens (r=-0.4043, P=0.0037). Values are shown as the mean ± standard errors of the mean based on three independent experiments. *P < 0.05, **P < 0.01, ****P < 0.0001

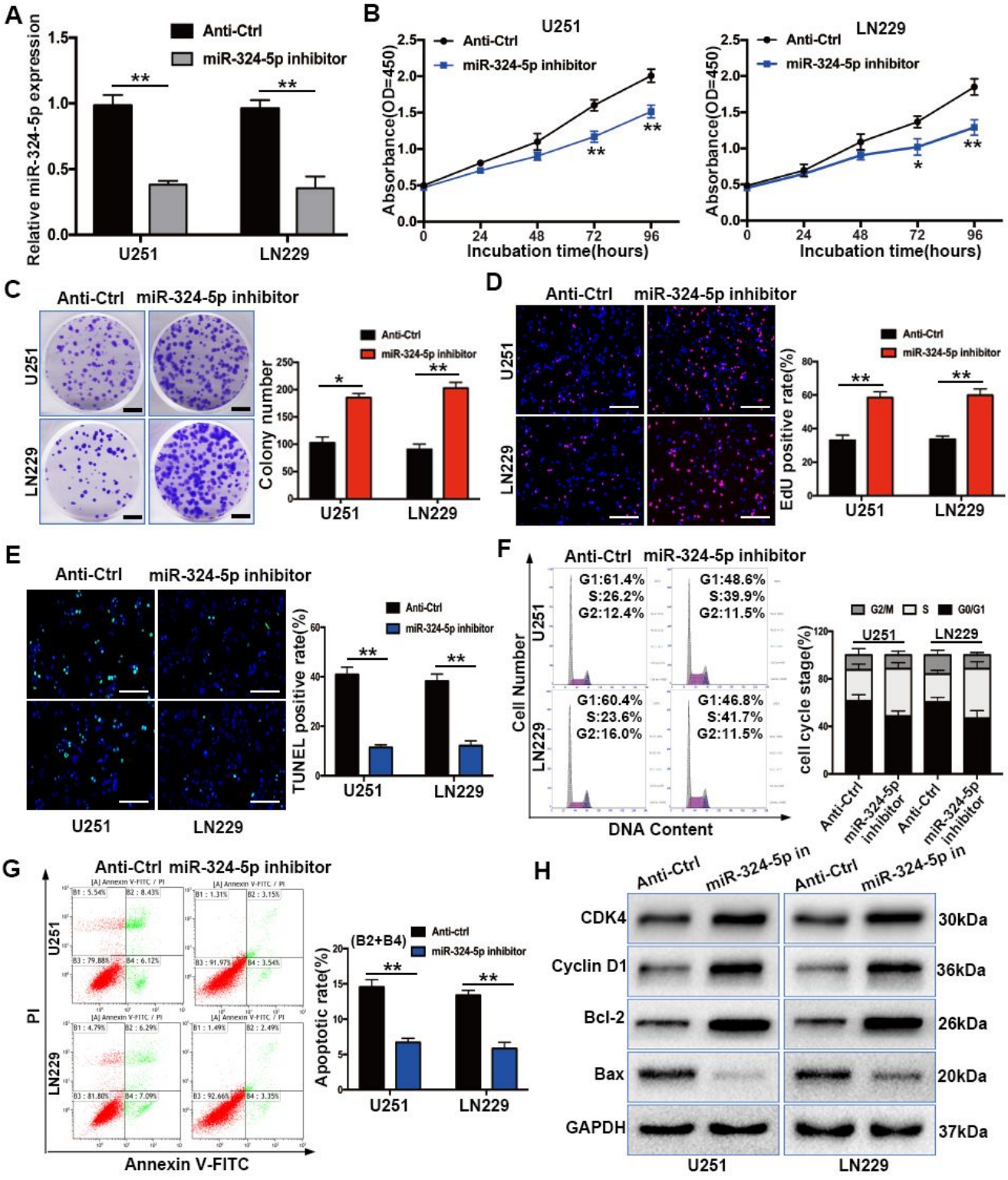

Figure 5

Effects of miR-324-5p on glioma cells proliferation, cell cycle, and apoptosis in vitro. A. The expression level of miR-324-5p was measured in U251 and LN229 cells transduced with the miR-324-5p inhibitor and their control groups by qRT-PCR. B. CCK-8 assays were used to determine the cell viability for miR-324-5p inhibitor transfected U251 and LN229 cells. C. Colony formation assay performed in U251 and LN229 cells after miR-324-5p suppression. scale bar=100μm D. Representative images of EdU assay using U251

and LN229 cells transfected with the miR-324-5p inhibitor or negative controls. scale bar=100μm E. The apoptosis efficiency of U251 and LN229 cells transfected with the control inhibitor or miR-324-5p inhibitor was detected by TUNEL analysis. scale bar=100μm F. The cell cycle phase of U251 and LN229 cells transfected with miR-324-5p inhibitor or negative control was analyzed by flow cytometry assay. G. FACS apoptotic assay performed in control or miR-324-5p suppressed U251 and LN229 cells. H. Western blot analysis of CDK4, Cyclin D1, Bcl-2 and Bax in U251 and LN229 cells after transfection of anti-Ctrl or miR-324-5p inhibitor. GAPDH was used as the loading control. Values are shown as the mean ± standard errors of the mean based on three independent experiments. *P < 0.05, **P < 0.01

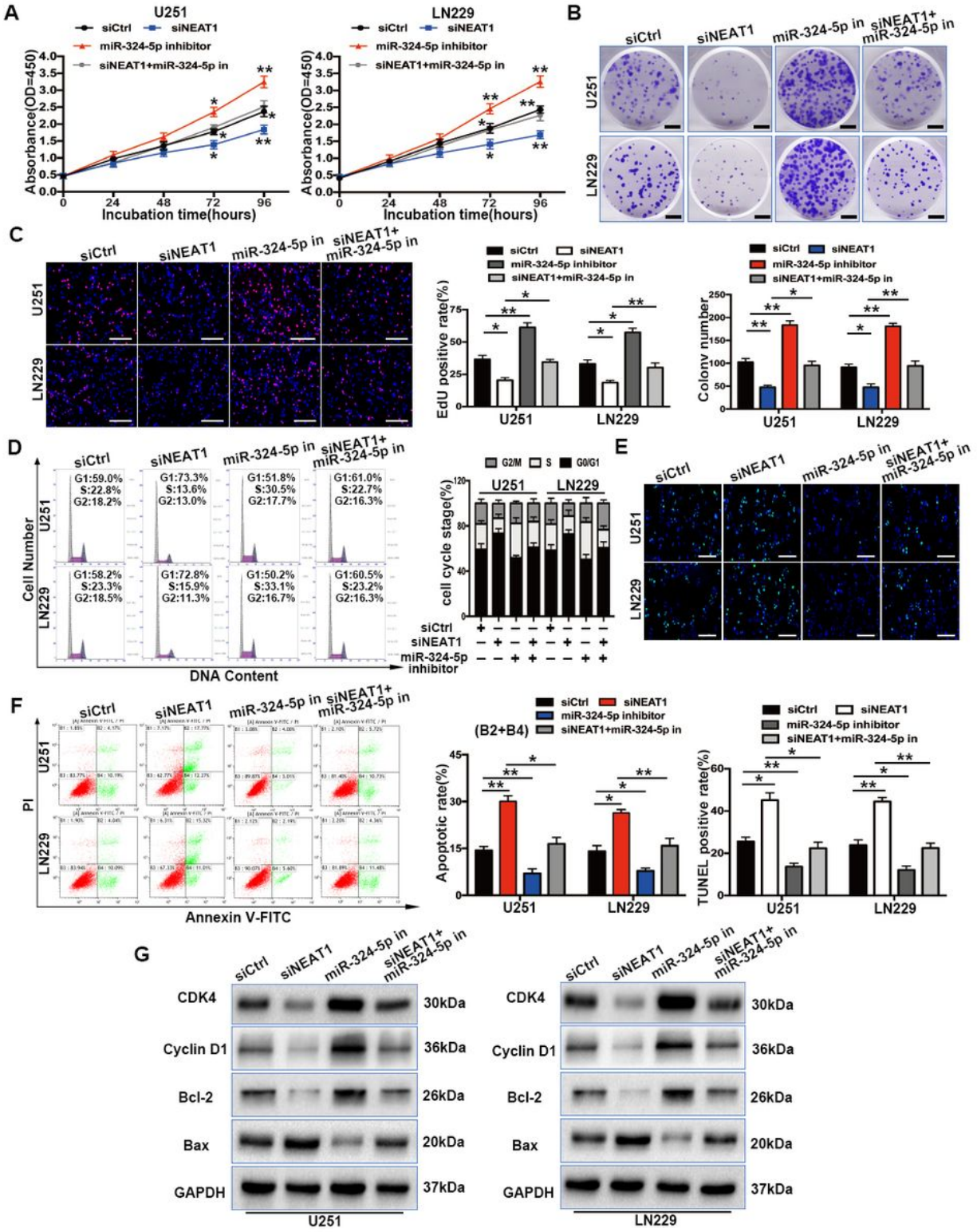

Figure 6

MiR-324-5p mediated the effects on glioma cells induced by NEAT1. A. The proliferation rate of glioma cells cultured in the NEAT1 silencing medium with and without miR-324-5p inhibitor by CCK-8 experiments. B. Representative images of colony formation assay using U251 and LN229 cells transfected with the indicated plasmids. scale bar=100μm C. The rescue experiments of EdU assay was performed on U251 and LN229 after co-transfected with siNEAT1, miR-324-5p inhibitor, or control siRNA.

scale bar=100μm D. The cell cycle distribution of siCtrl or siNEAT1-transduced U251 and LN229 cells by introducing knockdown of miR-324-5p. E. TUNEL assay with siCtrl or siNEAT1 transduced U251 and LN229 cells without transfection or transfected with miR-324-5p inhibitor. scale bar=100μm F. Apoptotic rates for U251 and LN229 cells after co-transfected with NEAT1, miR-324-5p inhibitor, or control siRNA were determined by Flow cytometry assays. G. Western blot analysis of CDK4, Cyclin D1, Bcl-2 and Bax in siCtrl or siNEAT1 cells after transfection of miR-324-5p inhibitor. GAPDH was used as the loading control. Values are shown as the mean ± standard errors of the mean based on three independent experiments. *P < 0.05, **P < 0.01

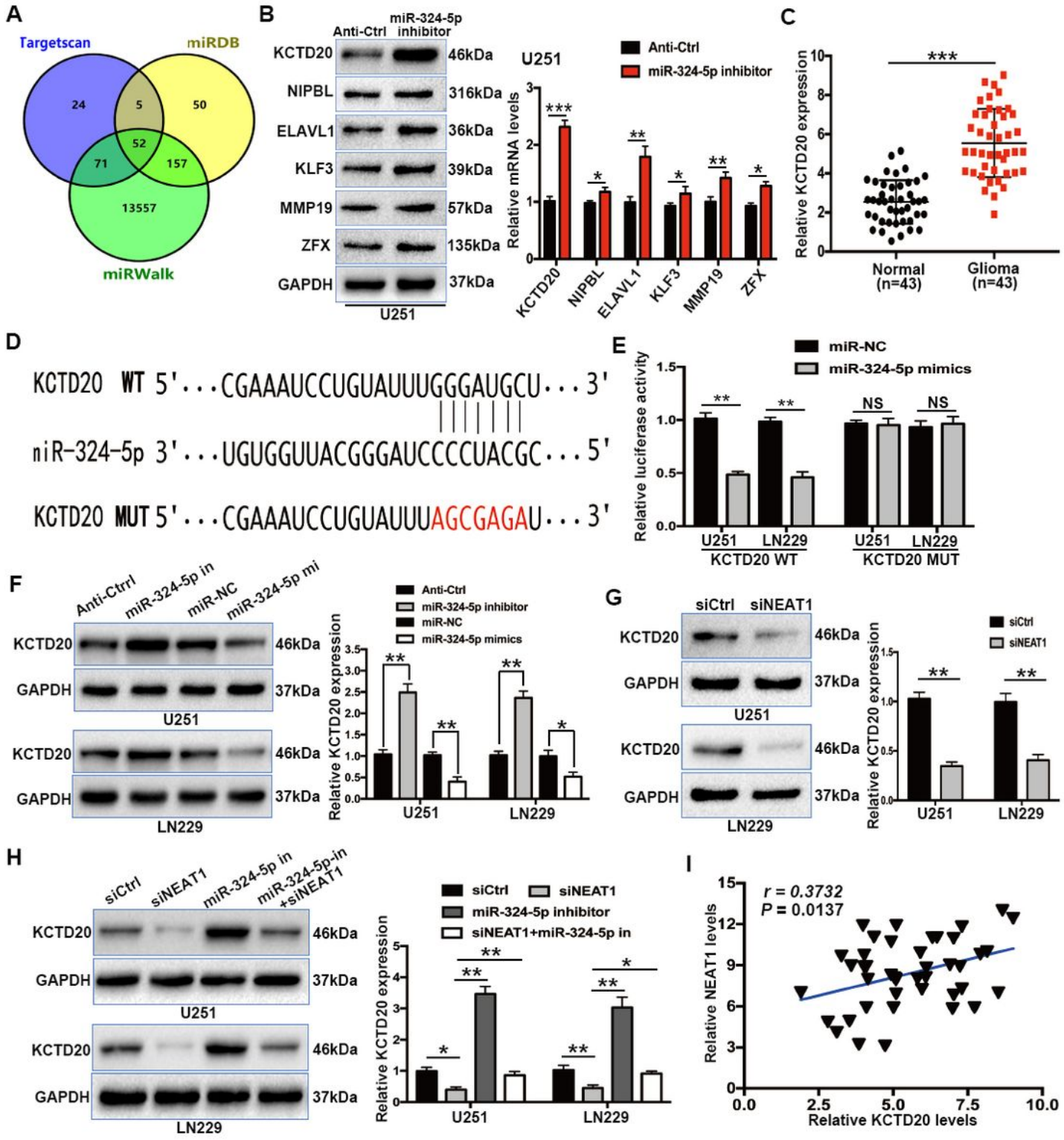

Figure 7

KCTD20 3'UTR is a direct target of miR-324-5p and is suppressed by the silencing of NEAT1. A. Three bioinformatics prediction software (Targetscan, miRBD and miRWalk) were used to search for target genes that can bound with miR-324-5p and displayed by Veen diagram. B. Effect of downregulated miR-324-5p expression on the level of 6 target genes (including KCTD20) measured by Western blot and qRT-PCR analysis. C. The expression level of KCTD20 was analyzed by qRT-PCR in glioma tissues and

corresponding adjacent non-tumor tissues (n=43). D. Predicted interactions between miR-324-5p and the 3'-UTRs of KCTD20 from Targetscan bioinformatics algorithm. E. The relative luciferase activity in cells co-transfected with wild type 3' UTR (KCTD20-WT) or mutant type 3' UTR (KCTD20-MUT) and indicated constructs miR-NC or miR-324-5p mimics, Renilla luciferase vector was used as an internal control. F. The protein and mRNA expression of KCTD20 in response to miR-324-5p inhibition group or miR-324 mimics group in U251 and LN229 cells glioma cells was evaluated by using Western blot and qRT-PCR assay. G. The KCTD20 protein and mRNA expression was analyzed after NEAT1 knockdown in U251 and LN229 cells. H. Western blot and qRT-PCR assays were used to determine the KCTD20 protein and mRNA expression of siNEAT1 and miR-324-5p inhibitor co-transfected U251 and LN229 cells. I. Scatter diagram exhibited a positive linear correlation of NEAT1 and KCTD20 in 43 paired glioma tissues by qRT-PCR ($r=0.3732$, $P=0.0137$). Values are shown as the mean ± standard errors of the mean based on three independent experiments. *$P < 0.05$, **$P < 0.01$, ***$P < 0.001$

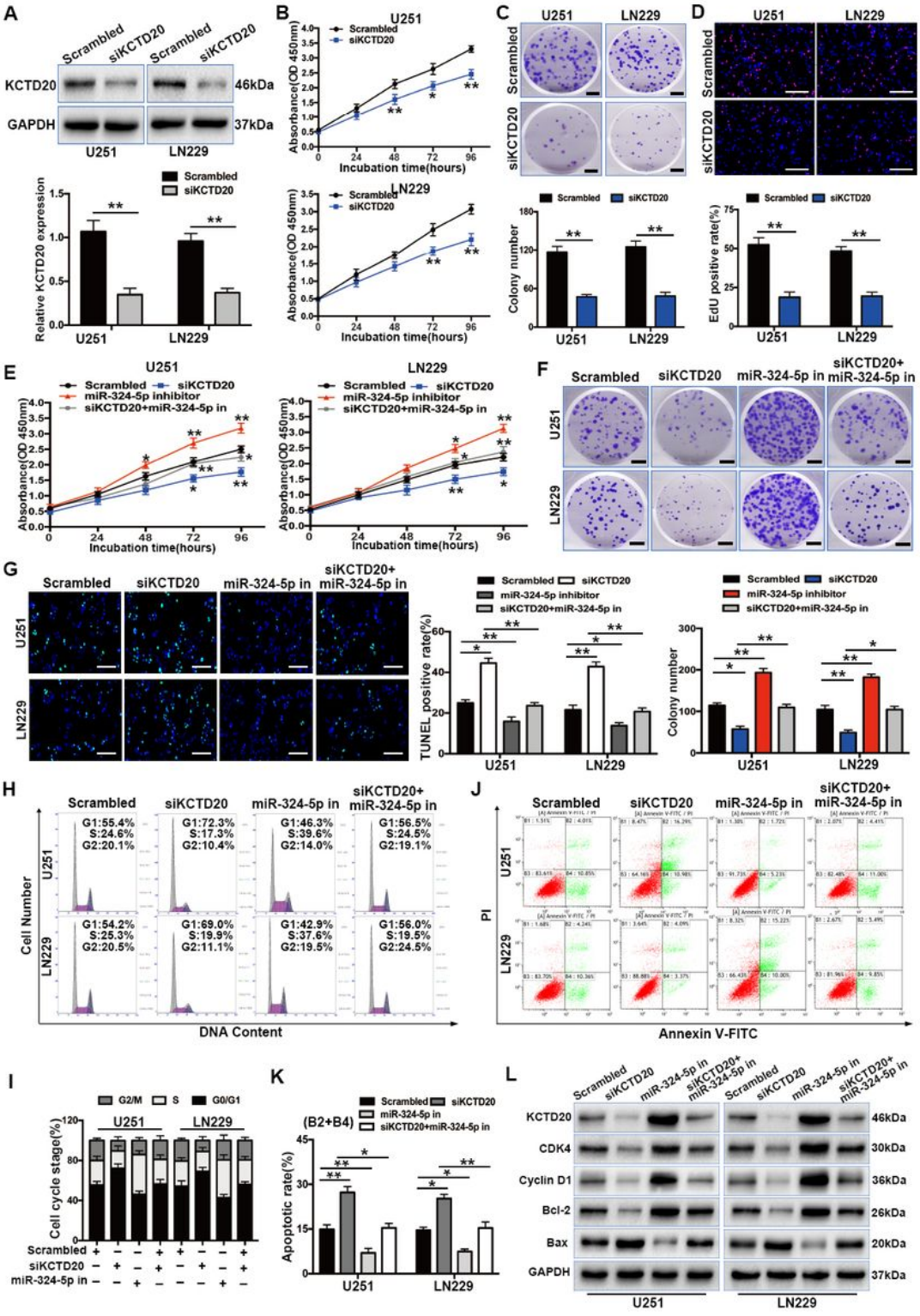

Figure 8

KCTD20 deletion inhibits cell proliferation and induced cell cycle arrest and promotes apoptosis in vitro. A. Western blot and qRT-PCR analysis of KCTD20 expression in U251 and LN229 cells after its suppression. B. CCK-8 assay measures the proliferation rate of cells after transfection with Scrambled or siKCTD20. C. Colonies grown from U251 and LN229 cells transfected with siKCTD20 or controls were counted. scale bar=100μm D. Representative images of EdU assay with U251 and LN229 cells

transfected with siKCTD20 or controls. scale bar=100μm E-F. The rescue experiment was performed after co-transfection with siKCTD20, miR-324-5p inhibitor, or corresponding control groups in U251 and LN229 cells. Cell proliferation efficiency were detected by CCK-8 and colony formation assay. scale bar=100μm G. Apoptotic rate was detected in the above U251 and LN229 cells using the TUNEL assay. H-I. Cell cycle distribution was measured in U251 and LN229 cells co-transfected with siKCTD20 and miR-324-5p inhibitor. J-K. Flow cytometry analysis and cell apoptotic rates in LN229 and U251 cells transfected with the indicated plasmid. L. Western blot analysis of KCTD20, cell cycle and apoptosis related proteins (CDK4, Cyclin D1, Bcl-2 and Bax), and GAPDH in U251 and LN229 cells transfected with siKCTD20, miR-324-5p inhibitor, or control groups. Values are shown as the mean ± standard errors of the mean based on three independent experiments. *P < 0.05, **P < 0.01

Supplementary Files

This is a list of supplementary files associated with this preprint. Click to download.

- SupplementaryMaterial.docx